# Supplementary Information

# Interfacial band bending and suppressing deep level defects via Eu-MOF mediated cathode buffer layer in MA-free inverted perovskite solar cell with high fill factor

*Tahir Imran*[a], *Hafiz Sartaj Aziz*[a], *Tayyaba Iftikhar*[b], *Munir Ahmad*[a], *Haibing Xie*[c], *Zhenghua Su*[a], *Yan Peiguang*[a], *Zonghao Liu*[d], *Guangxing Liang*[a,*], *Wei Chen*[d,*], *Shuo Chen*[a,*]

[a]Shenzhen Key Laboratory of Advanced Thin Films and Applications, Key Laboratory of Optoelectronic Devices and Systems of Ministry of Education and Guangdong Province, State Key Laboratory of Radio Frequency Heterogeneous Integration, College of Physics and Optoelectronic Engineering, Shenzhen University, Shenzhen 518060, China

[b]Guangdong Key Laboratory of Biomedical Measurements and Ultrasound Imaging, School of Biomedical Engineering, Shenzhen University Medical School, Shenzhen University, Shenzhen 518060, China

[c]Institute for Advanced Study, Shenzhen University, Shenzhen, Guangdong 518060, China

[d]Wuhan National Laboratory for Optoelectronics, Huazhong University of Science and Technology, Luoyu Road 1037, Wuhan, 430074, China

*Corresponding authors: Email: lgx@szu.edu.cn (Guangxing Liang); wnlochenwei@hust.edu.cn (Wei Chen); chensh@szu.edu.cn (Shuo Chen)

## Experimental section

### Materials

ITO substrate, Formamidine iodide (FAI, >99.5%), lead (II) iodide ($PbI_2$, >99.99%) Cesium iodide (CsI, >99.99%), [6,6]-Phenyl-C61-butyric acid methyl ester (PCBM) and [4-(3,6-dimethyl-9H-carbazol-9-yl)butyl]phosphonic acid (Me-4PACz) were procured from Advance election technology Crop. Europium nitrate ($Eu.NH_{3,}$ 99.9%) and 1,3,5-benzenetricarboxylic acid, (99.9%) were purchased from aladin. Ethyl acetate (EA 99.98%), isopropanol (IPA, 99.9%), Dimethyl sulfoxide (DMSO, 99.8%), N, N Dimethylformamide (DMF, 99.8%), Aluminum oxide nanoparticles (<50 nm, 20 wt % in isopropanol) and chlorobenzene (CB, 99.9%) were obtained from Sigma-Aldrich. Bathocuproine (BCP) was purchased from TCI chemicals.

### Synthesis of Eu-MOF

To synthesize Eu-MOF, a hydrothermal method was employed. Initially, 5.5 g of $Eu(NO_3)_3 \cdot 6H_2O$ was dissolved in 15 mL of deionized water to form Solution A. Separately, 1.76 g of 1,3,5-benzenetricarboxylic acid was dissolved in 60 mL of DMF to form Solution B. Solutions A and B were then combined, resulting in Solution C. This mixture was stirred and sonicated for half an hour to ensure complete dissolution of all components. The homogeneous Solution C was then transferred into a 100 mL Teflon-lined stainless steel autoclave. The autoclave was placed in an oven and heated to 120°C for 18 hours. After heating, the system was allowed to cool to room temperature. The resulting solid product was washed thoroughly with anhydrous ethanol to eliminate any impurities. This washing process included 5 cycles of centrifugation. Finally, the white solid crystals obtained and dried overnight at 60°C in a vacuum oven.

**Device fabrication**

First, the ITO substrates were sequential washed with deionized water, 95% ethanol, acetone, and 99% ethanol in an ultrasonic bath for 10 minutes. Subsequently, the ITO was UV-Ozone treated for 25-30 minutes. Following cooling, Me-4Pacz (1 mg $mL^{-1}$ in methanol) was spin-coated at 3000 rpm (ramp rate: 1000 rpm $s^{-1}$) for 30 seconds and then annealed at 90 °C for 12 minutes. After the substrates cooled down, an $Al_2O_3$ solution (25 µl in 1 mL IPA) was spin coated on the SAM layer as a modifier. The 1.5 mM $FA_{0.85}Cs_{0.15}PbI_3$ precursor solution was prepared by mixing FAI, CsI, and $PbI_2$ in anhydrous 4:1 = DMF:DMSO (v:v) and kept stirring for 12 hours at room temperature. Subsequently, 50 µL of PSK solution was used on top of $Al_2O_3$-treated Me-4PACz substrates (in a single-step coating), spun at 5500 rpm for 50 seconds and 3000 rpm. Additionally, 150 µL of ethyl acetate was dropped onto the substrates after 15 seconds of spinning. The substrates were quickly annealed, first at 110 °C for 5 minutes then for 20 minutes at 105 °C. For the additives-based precursor, a certain amount of additives was added. Then, PEACl solution (1 mg $mL^{-1}$ in IPA) was spin-coated at 6000 rpm for 25 seconds and annealed at 95 °C for 5 minutes. The PCBM (20 mg $mL^{-1}$ in chlorobenzene) was spin coated onto the PEACl layer at 2000 rpm (ramp rate: 3000 rpm $s^{-1}$) for 30 seconds. Later, an isopropanol-saturated solution of Eu-MOF:BCP with a 1:1 molar ratio was spin-coated on PCBM at 6000 rpm for 30 seconds and annealed at 70 °C for 10 minutes. At the end, a 105 nm copper cathode was thermally evaporated in a high vacuum chamber ($<8 \times 10^{-5}$ Pa) with a 0.09 $cm^2$ mask.

**Characterization and measurements**

X-ray photoelectron spectroscopy (XPS) analysis was conducted on PHI 5000 Versa Probe III instrument equipped with a monochromatic Al K$\alpha$ X-ray source. UV-Vis spectra of perovskite thin films were acquired using a Shimadzu UV-3600 UV/Vis/NIR spectrophotometer. The band

bending of Eu-MOF-modified thin films was investigated using ultraviolet photoelectron spectroscopy (UPS) with a He I source of 21.22 eV, employing the PHI 5000 Versa Probe. The current density-voltage (*J–V*) curves were assessed under AM 1.5 G simulated sunlight illumination (100 mW $cm^{-2}$) using a multimeter (Keithley, 2400 Series). External quantum efficiency (EQE) spectra were taken through the Zolix SCS101 system. The atomic force microscopy (AFM) micrographs of the corresponding thin films were observed using an NT-MDT Spectrum Instrument in semi-contact mode. To analyze both topography and surface potentials the kelvin probe force microscopy (KPFM) characterizations were conducted using a Dimension ICON system equipped with a gold-coated silicon cantilever. The growth orientation of the perovskite (PSK) thin film was investigated using X-ray diffraction (XRD) with an Ultima-iv diffractometer. All the scanning electron microscope (SEM) images related to PSCs were examined using SEM machine with a Zeiss SUPRA 55. To analyze the elemental distribution, SEM-coupled energy dispersive spectroscopy (EDS) was employed. The electrochemical impedance spectroscopy (EIS), transient photovoltage (TPV) and Mott-Schottky (*M–S*) measurements were performed via Zennium electrochemistry workstation (Zahner, Germany). The Cyclic voltammetry (CV) curves were measured with electrochemical workstation CHI660E.

**Table S1.** PV parameters of FACs-based devices with different $Pb(SCN)_2$ concentrations.

| **Concentration (%)** | $V_{OC}$ **(V)** | $J_{SC}$ **(mA cm$^{-2}$)** | **FF (%)** | **PCE (%)** | |
|---|---|---|---|---|---|
| | | | | **Average** | **Best** |
| Pristine | 1.12 | 25.44 | 83.12 | 22.91±0.84 | 23.70 |
| 1 | 1.12 | 25.47 | 83.15 | 22.95±0.21 | 23.75 |
| 2 | 1.13 | 25.64 | 84.12 | 23.85±0.42 | 24.40 |
| 3 | 1.11 | 25.09 | 81.14 | 21.61±0.24 | 22.63 |
| 4 | 1.08 | 23.55 | 78.33 | 18.72±0.63 | 19.92 |

**Table S2.** PV parameters of FACs-based devices without additive, 2% $Pb(SCN)_2$ additive, and 2% $Pb(SCN)_2$ together with a modified cathode buffer layer of Eu-MOF@BCP.

| Device(s) | $V_{OC}$ (V) | $J_{SC}$ (mA cm$^{-2}$) | FF (%) | PCE (%) | |
|---|---|---|---|---|---|
| | | | | Average | Best |
| Control | 1.12 | 25.44 | 83.12 | 22.91±0.65 | 23.70 |
| 2% $Pb(SCN)_2$ | 1.13 | 25.64 | 84.12 | 23.85±0.38 | 24.40 |
| 2% $Pb(SCN)_2$ , Eu-MOF@BCP | 1.14 | 25.85 | 85.11 | 24.56±0.38 | 25.11 |

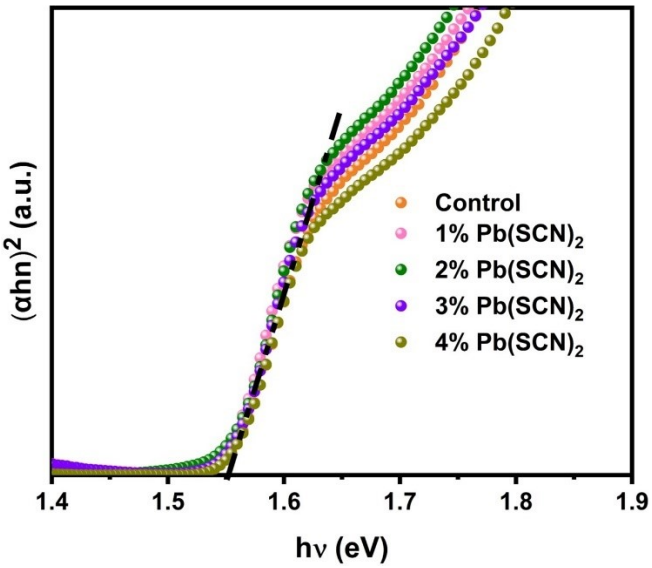


**Fig. S1** Tauc plot calculated from UV-Vis spectra of PSK thin films treated with various constructions of $Pb(SCN)_2$ additive.

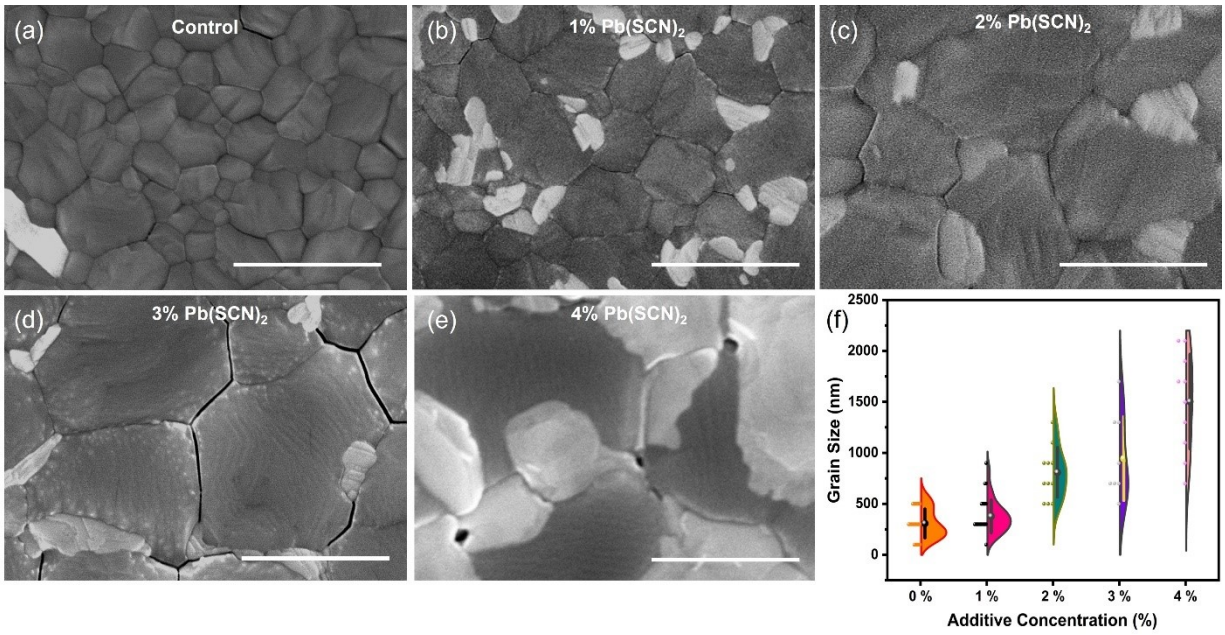


**Fig. S2** Top SEM images (a-e) and grain size distribution (f) of PSC thin films treated with various constructions of $Pb(SCN)_2$ additive.

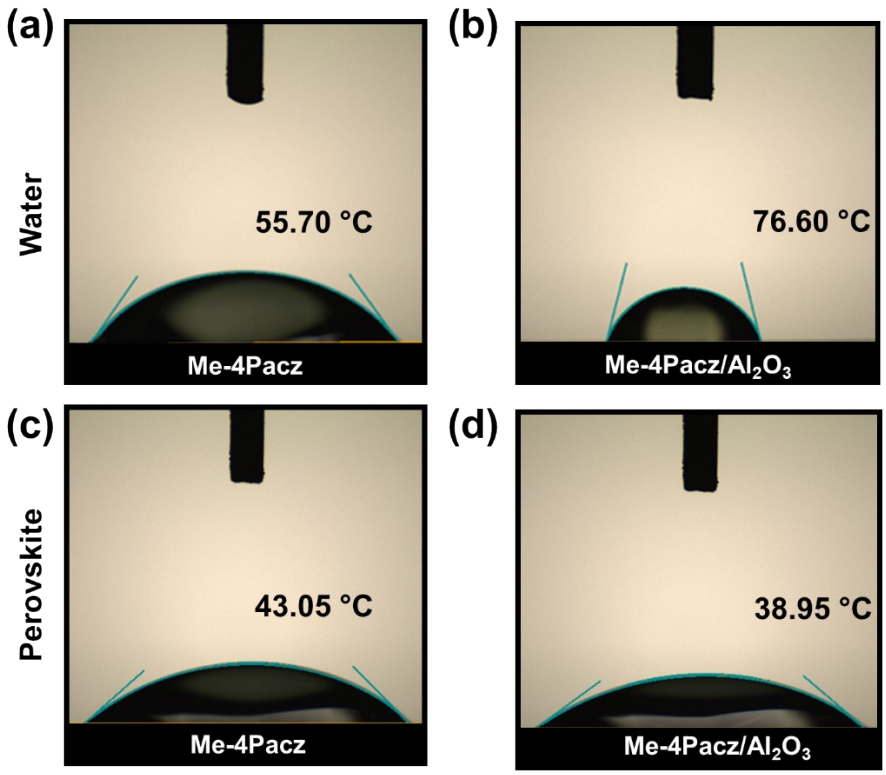


**Fig. S3** Water contact angle measurement on (a) Me-4PACz and (b) $Al_2O_3$ modified Me-4PACz surface and Perovskite ink contact angle measurement on (c) Me-4PACz and (d) $Al_2O_3$ modified Me-4PACz surface.

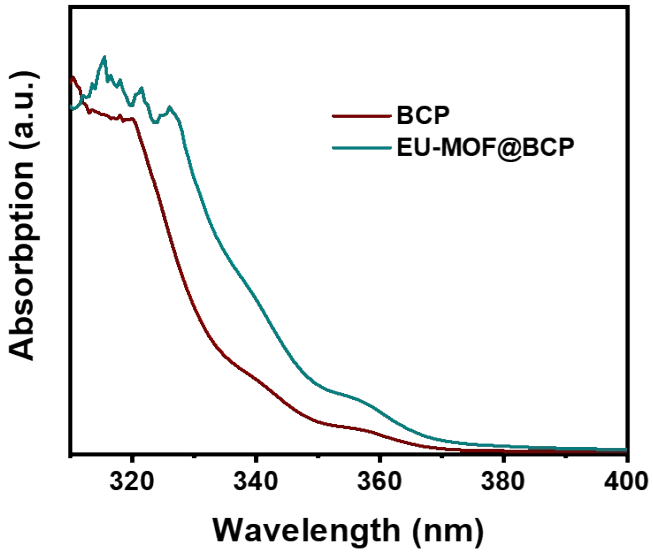


**Fig. S4** Normalized absorption spectra of BCP and Eu-MOF@BCP in toluene solution.

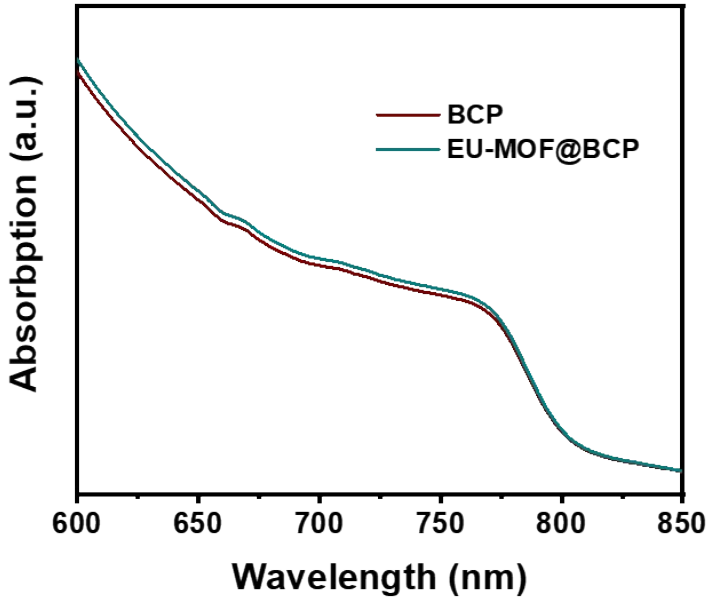


**Fig. S5** Normalized absorption spectra of BCP and Eu-MOF@BCP as top layer (full device) in toluene solution.

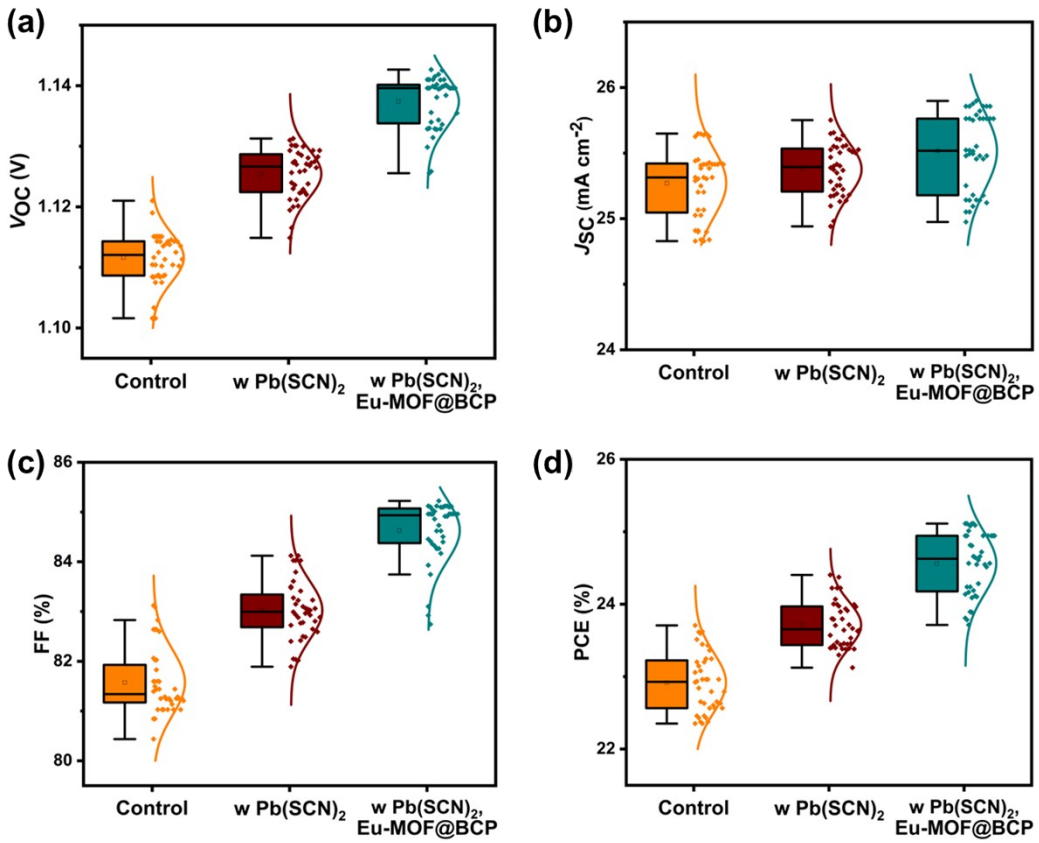


**Fig. S6** PV performance parameters of PSCs devices based on control, with $Pb(SCN)_2$ and with $Pb(SCN)_2$, Eu-MOF@BCP as CBL.

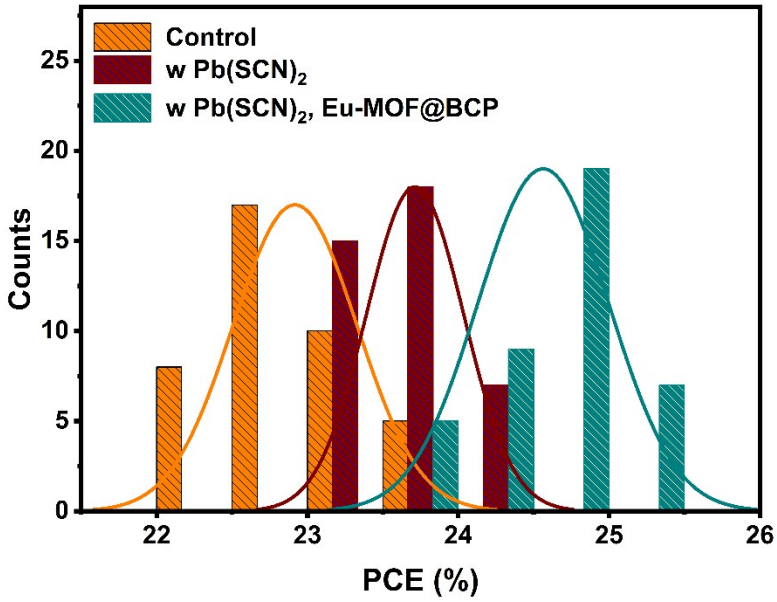


**Fig. S7** Performance histogram of PSCs devices based on control, with $Pb(SCN)_2$ and with $Pb(SCN)_2$, Eu-MOF@BCP as CBL.

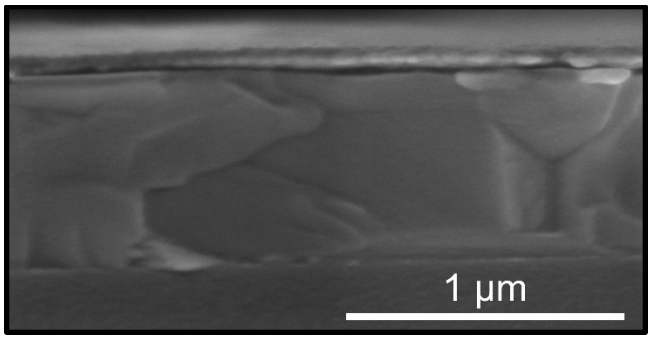


**Fig. S8** Cross section SEM image of champion device.

**Table S3.** Summary table of PV parameters of CBL engineering in inverted PSCs.

| **Year** | ***CBL*** | $V_{OC}$ **(V)** | $J_{SC}$ **(mA cm$^{-2}$)** | **FF (%)** | **PCE (%)** | **References** |
|---|---|---|---|---|---|---|
| 2027 | Rhodamine | 1.05 | 20.23 | 77.19 | 16.42 | 1 |
| 2021 | carbolong ligand | 1.07 | 23.84 | 83.52 | 21.29 | 2 |
| 2023 | RBH | 1.09 | 22.80 | 81.69 | 20.37 | 3 |
| 2023 | PNPDI | 1.18 | 23.46 | 78.20 | 21.46 | 4 |
| 2024 | NDI-ZI | 1.10 | 25.20 | 84.09 | 23.30 | 5 |
| 2024 | PDTI1 | 1.18 | 25.21 | 82.56 | 24.64 | 6 |
| 2024 | α-$In_2Se_3$ | 1.13 | 25.09 | 82.80 | 23.36 | 7 |
| **2024** | **Me-4PACz** | **1.14** | **25.85** | **85.11** | **25.11** | **This Work** |

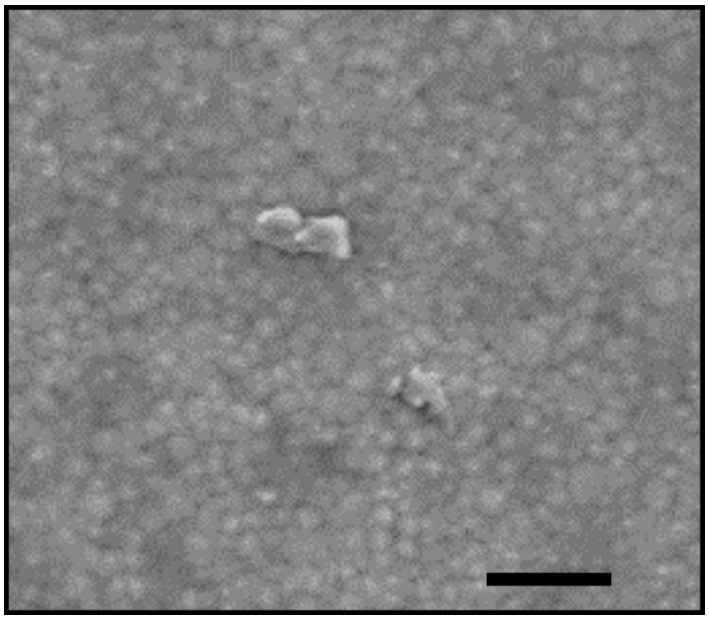

**Fig. S9** TOP SEM image of Eu-MOF@BCP as CBL.

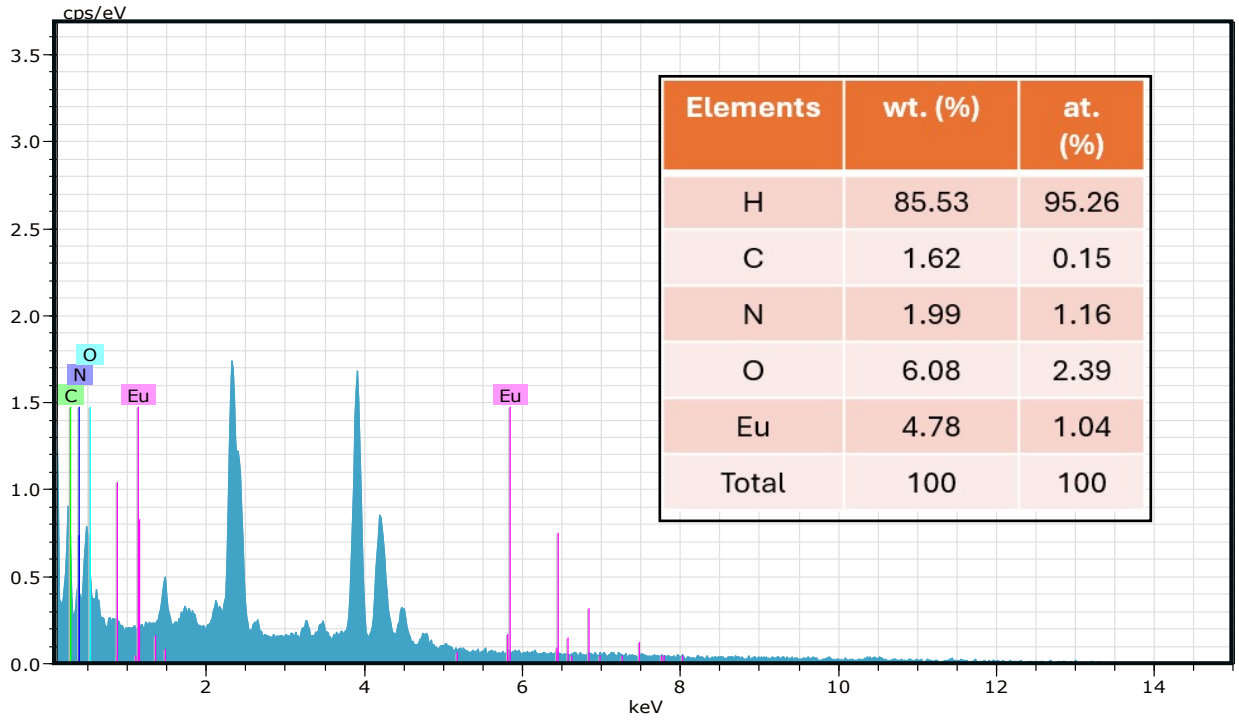


**Fig. S10** EDX analysis of PSC device with Eu-MOF@BCP as the top layer (taken from S9); inset shows the elemental distribution table.

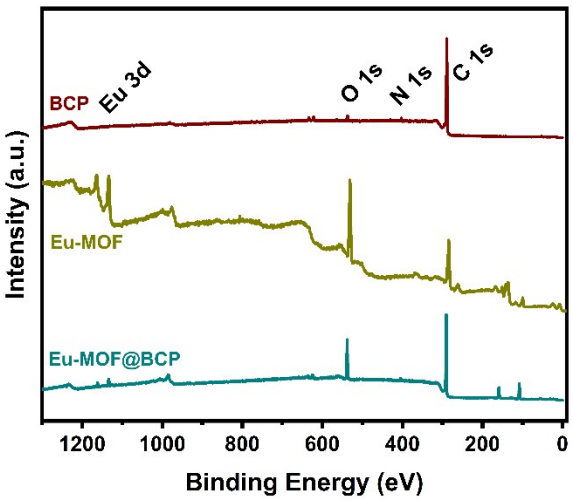


**Fig. S11** Comparison of full XPS spectra of BCP, Eu-MOF@BCP perovskite thin film devices with pure synthesized Eu-MOF powder.

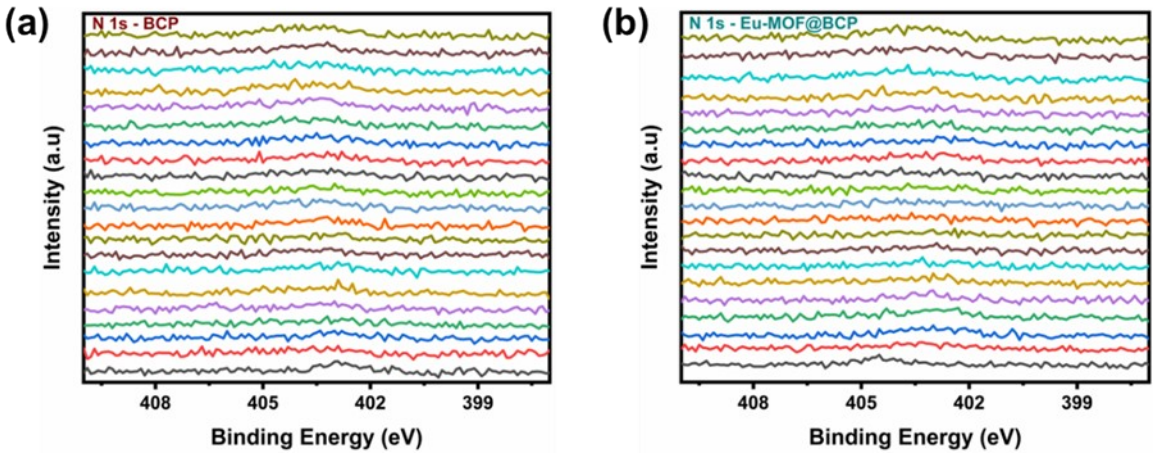


**Fig. S12** N 1s spectra of BCP and Eu-MOF@BCP PSCs up to 20nm depth.

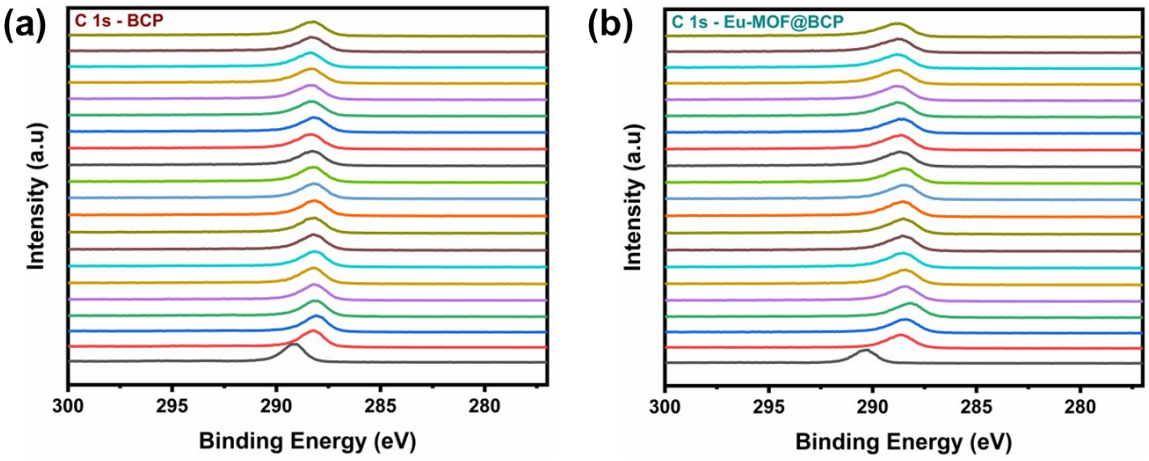


**Fig. S13** C 1s spectra of BCP and Eu-MOF@BCP PSCs up to 20 nm depth.

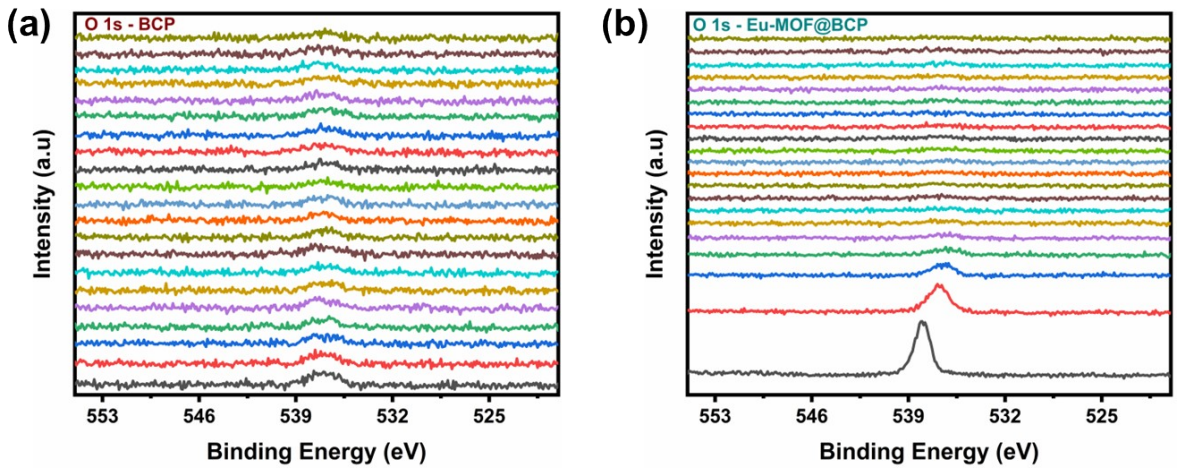


**Fig. S14** O 1s spectra of BCP and Eu-MOF@BCP PSCs up to 20nm depths.

**Table S4.** The TRPL values were obtained by fitting curves (Fig. 3d) for full devices fabricated with 0 % $Pb(SCN)_2$, 2% $Pb(SCN)_2$, and 2% $Pb(SCN)_2$ devices having Eu-MOF coupled BCP as ETL. The TRPL spectra were fitted by S1.1 equation and calculated by equation S1.2.

$$Y = A_1 \exp\left(-\frac{t}{\tau_1}\right) + A_2 \exp\left(-\frac{t}{\tau_2}\right) + y_0 \quad \text{(S1.1)}$$

$$\tau_{avg} = \frac{A_1\tau_1 + A_2\tau_2}{A_1 + A_2} \quad \text{(S1.2)}$$

Where $A_1$, $A_2$ are relative amplitudes and $\tau_1$, $\tau_2$ is the fast composite life and slow composite life, respectively, and Y represents the compensation coefficient.

| **Device configurations** | **$A_1$** | **$A_2$** | **$\tau_1$ (ns)** | **$\tau_2$ (ns)** | **$\tau_{ave}$ (ns)** |
|---|---|---|---|---|---|
| Control | 0.42 | 0.54 | 3.45 | 15.33 | 10.08 |
| 2% $Pb(SCN)_2$ | 0.61 | 0.35 | 2.16 | 9.84 | 4.94 |
| 2% $Pb(SCN)_2$ / Eu-MOF@BCP | 0.69 | 0.27 | 1.81 | 6.56 | 3.15 |

**SCLC measurement:**

For the SCLC measurement in the dark, the $N_t$ value was determined by utilizing Equation S1.3.

$$N_t = \frac{2\varepsilon_0 \varepsilon V_{TFL}}{qL^2} \quad \text{(S1.3)}$$

In this equation, $\varepsilon_0$ represents the vacuum permittivity, L denotes the thickness of the perovskite film, and q represents charge on an electron. The ε represents the relative dielectric constant. In SCLC measurement a scan rate of 50 mV/s with a direction from −200 mV to 1.2 V were used.

## Notes and references


1. J. Ciro, S. Mesa, J. I. Uribe, M. A. Mejía-Escobar, D. Ramirez, J. F. Montoya, R. Betancur, H.-S. Yoo, N.-G. Park and F. Jaramillo, Nanoscale, 2017, **9**, 9440-9446.
2. J. Wang, J. Li, Y. Zhou, C. Yu, Y. Hua, Y. Yu, R. Li, X. Lin, R. Chen, H. Wu, H. Xia and H.-L. Wang, J. Am. Chem. Soc., 2021, **143**, 7759-7768.
3. N. Liu, J. Xiong, G. Wang, Z. He, J. Dai, Y. Zhang, Y. Huang, Z. Zhang, D. Wang, S. Li, B. Liu, X. Deng, H. Zhang and J. Zhang, Adv. Funct. Mater., 2023, **33**, 2300396.
4. D. Wang, C. Kang, T. Ye, D. He, S. Jin, X. Zhang, X. Sun and Y. Zhang, J. Energy Chem., 2023, **82**, 334-342.
5. Y. W. Noh, J. M. Ha, J. G. Son, J. Han, H. Lee, D. W. Kim, M. H. Jee, W. G. Shin, S. Cho, J. Y. Kim, M. H. Song and H. Y. Woo, Mater. Horiz., 2024, **p**, p.
6. L. Gao, H. Wang, Q. Guo, Z. Wang, F. Yuan and E. Zhou, Chem. Eng. J., 2024, **480**, 148277.
7. H. Zhang, W. Liu, Y. Bao, R. Wang, J. Liang, L. Wan and H. Wang, J. Mater. Chem., 2024, **12**, 7577-7586.